PHYSICAL REVIEW E **72**, 045106(R) (2005)

Fragment velocity distribution in the impact disruption of thin glass plates

Toshihiko Kadono,[1,*] Masahiko Arakawa,[2] and Noriko K. Mitani[3]
[1]*Institute for Research on Earth Evolution, Japan Agency for Marine-Earth Science and Technology, Kanagawa 236-0001, Japan*
[2]*Institute of Low Temperature Science, Hokkaido University, Sapporo 060-0819, Japan*
[3]*Earthquake Research Institute, University of Tokyo, Tokyo 113-0032, Japan*
(Received 19 April 2005; revised manuscript received 25 August 2005; published 27 October 2005)

We present the experimental results of the measurement of fragment velocity in an impact disruption. Cylindrical projectiles impact on a side (edge) of thin glass plates, and the dispersed fragments were observed using a high-speed camera. The fragment velocity did not depend on the mass but rather on the initial position of the fragment; the velocity component parallel to the projectile direction increased with the distance from the impacted side, while the component perpendicular to the projectile direction increased with the distance from the central axis parallel to the projectile direction. It appears that there are two mechanisms for fragment ejection: one is "spallation," where the fragment velocities depend on the particle velocity induced by shock waves, and the other is "elastic ejection," where the velocities are controlled by the strain energy stored in targets and are at most a few tens of meters per second. We performed a one-dimensional numerical simulation of elastic ejection with a discrete element method and obtained the velocity distribution as a function of the initial position. The numerical results are qualitatively consistent with the experimental ones.

DOI: 10.1103/PhysRevE.72.045106 PACS number(s): 46.50.+a, 62.20.Mk, 96.35.Cp

Fragmentation of brittle solids has been investigated for many decades in various fields of science and engineering [1,2]. In recent years, our understanding of fragment mass distributions has improved [3–7]. On the other hand, another important feature—fragment velocity—is still not fully understood, although it is important for partitioning of the impact energy, which is the most fundamental quantity for understanding the whole process of fragmentation. In planetary science, fragment velocity has been studied in order to clarify the origin of asteroid families and the process of planetesimal accretion [2,8–14], but fragment velocity data from disruption experiments are still sparse, and are limited to the velocities of selected fragments. Thus some basic problems still remain. For example, one important question is whether or not the velocity of the fragment depends on its mass. Nakamura and Fujiwara [13] obtained the results that the fragment velocity was expressed as the $-1/6$ power of the fragment mass, while Giblin *et al.* [14] found considerable variation in the slope of the fragment size-velocity distribution.

One of the reasons for the paucity of data is that the measurements of fragment mass and velocity are difficult when spherical or cubic targets are disrupted. Fragments overlap each other in the line of sight, such that some fragments are not visible. Also, because it is difficult to determine the shape of the fragments, the volume and mass can not be estimated precisely. Moreover, although in principle it is possible to obtain three components of the fragment velocities using two cameras, in actual practice it is quite difficult to identify fragments in two images recorded by different cameras in different directions. As a result, the number of fragments whose mass and velocity can be determined was so small that the statistical discussion was difficult.

Here we consider the impact fragmentations of thin glass plates. Projectiles impact on one side (edge) of the glass plates. In this case, the displacements of fragments were limited to the plate plane, and hence we were able to observe the velocity and mass (area) of most fragments with a high-speed camera.

The experimental system is shown in Fig. 1(a) [15]. Thin Pyrex glass plates (square) with a thickness of 1 mm and a side length of 30, 50, 100, or 200 mm were vertically installed and suspended by two fine threads under an ambient pressure of 1 atmosphere. Cylindrical aluminum projectiles with a diameter of 15 mm and a height of 10 mm, which

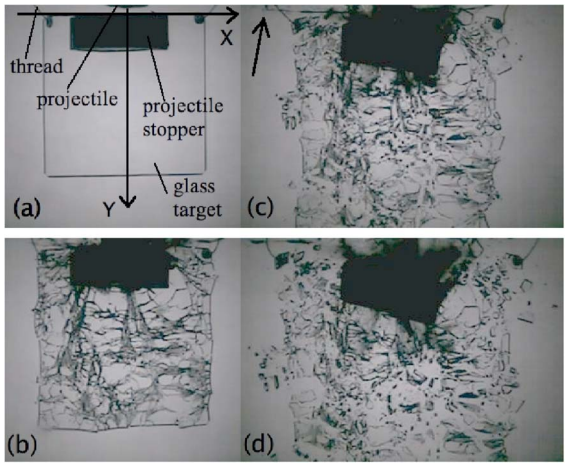

FIG. 1. (Color online) Consecutive images in the experiments using a glass plate with a side of 50 mm. The projectile impacted against the center of the upper side from the top at an impact velocity of 65.4 m/s. (a) Just before the impact. The coordinate system used in this paper is shown. (b) Just after the impact [0.25 ms after (a)]. (c) 0.5 ms after (b). The arrow indicates "jet." (d) 1 ms after (b).

*Author to whom correspondence should be addressed. FAX: 81-4-7136-3932. Electronic address: kadono@jamstec.go.jp

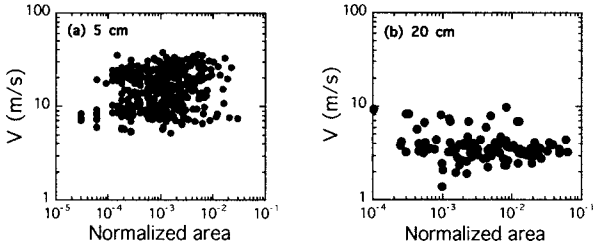

FIG. 2. The fragment velocity V against the fragment area for (a) 50-mm and (b) 200-mm targets. The fragment area is normalized by the initial target area.

were accelerated by an air gun at the Institute of Low Temperature Science, impacted against the upper side of the targets from the top with an impact velocity of 52.3–73.2 km/s. Around the impact point, two brass semicircular projectile stoppers with a radius of 15 mm and a thickness of 10 mm were set to prevent the projectile from penetrating into the target. These stoppers were connected by two thin threads and hooked on the upper side of the target. The projectile initially impacted the target, and its motion was quickly terminated by the stoppers. A total of five shots were carried out (one shot for the 30-, 50-, and 200-mm targets and two shots for the 100-mm targets).

Fragment motion was observed using a high-speed video camera with a framing speed of 4000 frames per second and an exposure time of 10 μs. Most experiments were carried out using a shadow photograph lighting system, except the experiment with a 200-mm target, which was done with a reflection lighting system. The camera view was normal to the target plane.

Figure 1 shows the result of the experiment using a glass plate with a side length of 50 mm. The projectile impacted against the center of the upper side from the top at an impact velocity of 65.4 m/s. (a) Just before the impact. The projectile is just visible at the top of the frame. The coordinate system used in this paper is shown; the X axis and Y axis are perpendicular and parallel to the projectile direction, respectively. (b) Just after the impact [0.25 ms after the image in Fig. 1(a)]. It can be seen that a number of cracks have been generated and the fragments have already moved. (c) 0.5 ms after the image in Fig. 1(b). Very fast fragments are observed (arrow). These are probably "jet," very fine and fast fragments thrown out during the earliest stage of the impact process, when the projectile first contacts the target [16]. (d) 1 ms after the image in Fig. 1(b). The fragments have flown away.

The positions of the fragments in each frame were measured, and the components of fragment velocities V_x and V_y were estimated. Figure 2 shows fragment velocity $V = \sqrt{V_x^2 + V_y^2}$ against the fragment area using the results obtained with (a) 50-mm and (b) 200-mm targets, respectively. The fragment area is normalized by the initial target area. The jet is not included. It seems in both cases that the dispersion of fragment velocities is large and that there is no one-to-one relation between the fragment area and velocity.

Figure 3 shows the velocity vectors drawn from their initial positions for (a) 50-mm and (b) 200-mm targets. The scale bar at the bottom right of each figure represents

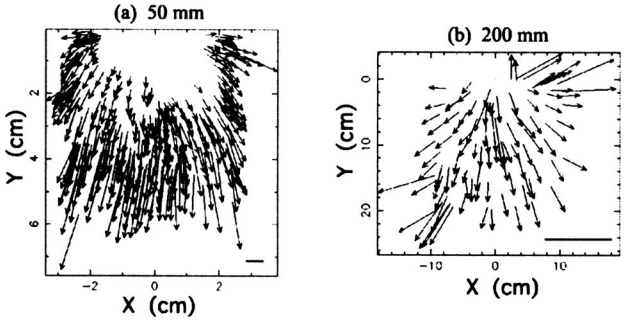

FIG. 3. Velocity vectors drawn from their initial positions for (a) 50-mm and (b) 200-mm targets. The scale bars at the bottom right of the figures represent 10 m/s in both cases. There are no vectors around the impact point due to the projectile stoppers.

10 m/s. We cannot plot vectors around the impact point because the initial positions of the fragments from there are not known due to the projectile stoppers. It seems that the fragment velocity depends on the initial position of fragments. For example, the absolute value of V_x is small around the Y axis and increases with the distance from the Y axis, and V_y, which is small around the impact point, increases with the distance from the X axis and reaches a maximum near the far side of the targets.

In Fig. 4, V_x and V_y for (a) 50-mm and (b) 200-mm targets are plotted as a function of x_0 and y_0, respectively, where x_0 and y_0 are the initial positions of fragments. One of the characteristic features is that there appear to be positive correlations in both cases; V_x and V_y increase with x_0 and y_0, respectively [17,18]. Another feature is that, for a 50-mm target [Fig. 4(a)], the V_y of most fragments is positive, and the maximum of V_y is larger than that of V_x (these features are seen in the results of 30- and 50-mm targets), while for a

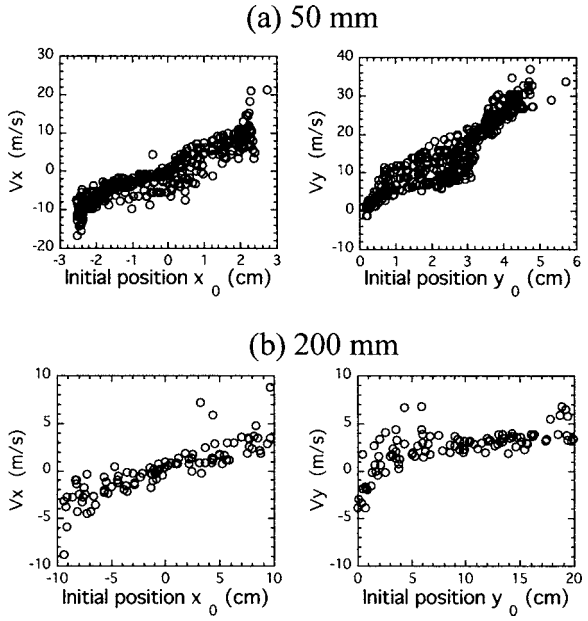

FIG. 4. Velocity components as a function of the initial position for (a) 50-mm (left: V_x; right: V_y) and (b) 200-mm (left: V_x; right: V_y) targets.

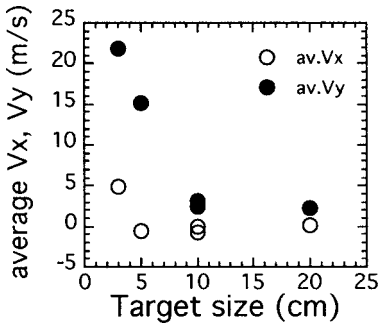

FIG. 5. The averages of V_x and V_y as a function of the side length of targets. The average of V_x is almost zero and V_y decreases with target size.

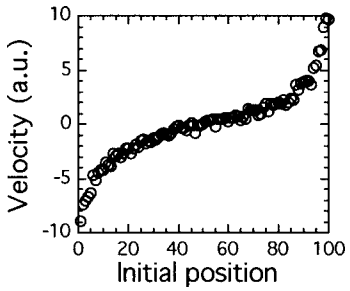

FIG. 6. Numerical results with DEM. The velocities of the particles are plotted against their initial positions. The velocities increase according to the initial position.

200-mm target [Fig. 4(b)], there are some fragments with negative V_y and the maxima of V_x and V_y are comparable (these features can also be seen in the results of the experiments using the 100-mm targets). Figure 5 shows the averages of V_x and V_y as a function of the target size. The average of V_x is almost zero in every case, while that of V_y is large for smaller (30- and 50-mm) targets and becomes small and comparable with that of V_x for larger (100- and 200-mm) ones.

In general, the shock waves generated by impacts are reflected from the sides of targets back into the interiors of targets as tensile waves (rarefaction waves). When the tensile stress is sufficiently large, the targets fail and "spall" fragments fly off [19]. The velocity of spall fragments is approximately twice the particle velocity induced by the shock waves. For the smaller targets, shock and rarefaction waves would be strong at the sides, and spallation is expected to occur. Since the projectile diameter and the target lengths are comparable, the stress distribution in the targets is nearly one-dimensional and the particle velocity and stress in the Y direction are larger. Hence the maximum velocity of V_y for small targets is probably larger than that of V_x.

When the target size increases, shock waves propagate radially in the targets and attenuate due to some factors such as the geometrical effect, crack formations, and rarefaction waves, before arriving at the sides. As a result, spall fragmentation does not occur, and fragments are ejected using stored elastic energy after outer adjacent fragments move away ("elastic ejection"). In this case the crack formation continues for approximately a few tens of microseconds [7], during which the elastic waves repeatedly propagate back and forth in the targets. Thus the stress distribution becomes nearly uniform in the targets, so that the maxima of V_x and V_y become comparable. It is noteworthy that the average velocity of fragments can be estimated to be at most a few tens of meters per second regardless of the impact velocity [20]. This is consistent with the experimental results for large targets. It should also be noted that, even in the experiments using small targets, not all fragments are ejected by spallation, and fragments in the inner parts are ejected by elastic ejection.

Next, in order to indicate that the elastic ejection also result in the dependence of the fragment velocity on the initial position as shown in Fig. 4 (the outer fragments move faster and the inner ones move slower), we carry out a one-dimensional numerical simulation using a discrete element method (DEM) with a soft particle model [21]. We consider 100 elastic particles with equal diameter as fragments, which are lined up in a row. Particles (fragments) are initially in contact with their adjacent fragments, but the distance between them is random rather than uniform. This means that the fragments store random elastic energy before ejection. After the release the fragments are accelerated using the elastic energy. At a certain time point, the fragment velocity is measured. Figure 6 shows the results. The fragments near the free boundaries move faster and that the velocities increase according to the initial position. This is consistent with the experimental results. This feature can be explained qualitatively as follows. The fragments begin to move after the release wave from the nearer free boundary arrives, and are accelerated in the direction to the nearer boundary. However, if the fragments initially exist around the center of the row, the release wave from the other boundary may arrive during the acceleration. As a result, these inner fragments are also accelerated in the opposite direction; the acceleration to the nearer boundary decreases. Thus the inner fragments have lower velocities. It should be noted that realistic two- or three-dimensional numerical simulations should be carried out for more quantitative discussion.

In summary, fragmentation experiments were carried out using thin glass plates, and the velocity of fragments was investigated. The results suggested that there was no one-to-one relation between the velocity and area (mass) of fragments, and that the velocity was dependent on the initial position of fragments; V_y increases with the distance between the initial position of fragments and the X axis, and V_x increases with the distance between the initial position and the Y axis. It appears that there are two mechanisms for fragment ejection: spallation and elastic ejection. We performed a one-dimensional numerical simulation of the elastic ejection and obtained the velocity as a function of initial position. The numerical results qualitatively agreed with the experimental ones.

The authors would like to thank A. M. Nakamura, O. S. Barnouin-Jha, and S. Sugita for their helpful comments.

[1] *Statistical Models for the Fracture of Disordered Media*, edited by H. J. Hermann and S. Roux (North-Holland, Amsterdam, 1990).

[2] A. Fujiwara, P. Cerroni, D. Davis, E. Ryan, M. Di Martino, K. Holsapple, and K. Housen, in *Asteroid II*, edited by R. P. Binzel, T. Gehrels, and M. S. Matthews (University of Arizona Press, Tucson, 1989), pp. 240–265.

[3] J. A. Aström, F. Ouchterlony, R. P. Linna, and J. Timonen, Phys. Rev. Lett. **92**, 245506 (2004); J. A. Aström, R. P. Linna, J. Timonen, P. F. Moller, and L. Oddershede, Phys. Rev. E **70**, 026104 (2004); R. P. Linna, J. A. Aström, and J. Timonen, *ibid.* **72**, 015601 (2005).

[4] F. Wittel, F. Kun, H. J. Herrmann, and B. H. Kröplin, Phys. Rev. Lett. **93**, 035504 (2004); Phys. Rev. E **71**, 016108 (2005).

[5] H. Katsuragi, D. Sugino, and H. Honjo, Phys. Rev. E **68**, 046105 (2003); **70**, 065103 (2004).

[6] T. Kadono, Phys. Rev. Lett. **78**, 1444 (1997).

[7] T. Kadono and M. Arakawa, Phys. Rev. E **65**, 035107 (2002).

[8] A. Fujiwara and A. Tsukamoto, Icarus **44**, 142 (1980); A. Fujiwara, *ibid.* **70**, 536 (1987).

[9] T. Waza, T. Matsui, and K. Kani, J. Geophys. Res. **90**, 1995 (1985).

[10] M. Arakawa, N. Maeno, M. Higa, Y. Iijima, and M. Kato, Icarus **118**, 341 (1995); M. Arakawa and M. Higa, Planet. Space Sci. **44**, 901 (1996); M. Arakawa, Icarus **142**, 34 (1999).

[11] I. Giblin, G. Martelli, P. N. Smith, A. Cellino, M. Di Martino, V. Zappala, P. Farinella, and P. Paolicchi, Icarus **110**, 203 (1994); I. Giblin, Planet. Space Sci. **46**, 921 (1998); I. Giblin, D. R. Davis, and E. V. Ryan, Icarus **171**, 487 (2004).

[12] A. Nakamura, K. Suguiyama, and A. Fujiwara, Icarus **100**, 127 (1992); A. Nakamura, A. Fujiwara, and T. Kadono, Planet. Space Sci. **42**, 1043 (1994).

[13] A. Nakamura and A. Fujiwara, Icarus **92**, 132 (1991).

[14] I. Giblin, G. Martelli, P. Farinella, P. Paolicchi, M. Di Martino, and P. N. Smith, Icarus **134**, 77 (1998).

[15] Previous studies have employed similar experimental systems in which a high-velocity projectile impacts on the side of plate-like targets [6,7]. See also a sketch shown in Fig. 1 of Ref. [7], which is the same system as used in the present paper.

[16] "Jetting" is known as one of the fragment ejection mechanisms [e.g., H. J. Melosh, *Impact Cratering: A Geologic Process* (Oxford University Press, New York, 1989)]. Since it has been often investigated, we do not discuss it in detail in this paper.

[17] In the disruption of basalt spheres and cubes, fragments from the original surface were also observed to have higher velocities [8,13].

[18] The correlations are recognized only in the combinations of V_x-x_0 and V_y-y_0 and there seems to be no correlation in the other combinations, such as V_x-y_0 and V_y-x_0.

[19] See, e.g., H. Kolsky and D. Rader, in *Fracture*, edited by H. Liebowitz (Academic Press, New York, 1968), pp.533–569.

[20] We can estimate the average fragment velocity as described in Ref. [9], assuming that the elastic energy $\sim E\varepsilon^2 m/\rho$, where E, ε, m, and ρ are the modulus of elasticity (e.g., Young modulus), strain, density, and fragment mass, respectively, is equal to the kinetic energy, $\sim mV^2 : E\varepsilon^2 m/\rho \sim mV^2$. This becomes $V \sim (E/\rho)^{1/2}\varepsilon \sim C\varepsilon$, where C is sound velocity of target materials. Since C of brittle materials such as glass and rocks is approximately kilometers per second and the maximum strain of these materials is $\sim 1\%$, V becomes approximately a few tens of meters per second regardless of the impact velocity. This is consistent with our experimental results, and similar to the results using basalt targets at an impact velocity of a few kilometers per second [8,13] and ice ones at a few hundreds of meters per second [10].

[21] See, e.g., P. A. Cundall and O. D. L. Strack, Geotechnique **29**, 47 (1979).